

## Tutorial

Chloë Nicholson-Smith, George K. Knopf\* and Evgueni Bordatchev\*

# Parametric analysis of thin multifunctional elastomeric optical sheets

<https://doi.org/10.1515/aot-2018-0012>

Received February 4, 2018; accepted April 12, 2018; previously published online May 16, 2018

**Abstract:** Flexible optical sheets are thin large-area polymer light guide structures that can be used to create innovative passive light-harvesting and illumination systems. The optically transparent micro-patterned polymer sheet is designed to be draped over arbitrary surfaces or hung like a curtain. The light guidance sheet is fabricated by bonding two or more micro-patterned layers with different indices of optical refraction. By imprinting micro-optical elements on the constituent layers, it is possible to have portions of the optical sheet act as a light concentrator, near ‘lossless’ transmitter, or diffuser. However, the performance and efficiency of the flexible optical sheet depends on the overall curvature ( $\kappa$ ) of the optical sheet and the relative orientation of incident light source. To illustrate this concept, the impact of key design parameters on the controlled guidance of light through a two-layer polydimethylsiloxane (PDMS) concentrator-transmitter-diffuser optical sheet is investigated using ray tracing simulation software. The analysis initially considers a flat ( $\kappa=0$ ) PDMS optical sheet exposed to a collimated light source. The impact of sheet curvature ( $\kappa>0$ ) on both system efficiency and illumination uniformity is then briefly explored. Critical design guidelines for creating multifunctional monolithic optical sheets are also summarized.

**Keywords:** concentrators; diffusers; elastomeric optics; large area optical sheets; polydimethylsiloxane; ray tracing simulation.

## 1 Introduction

Optical sheets are an emerging technology that enables a wide variety of large-area ( $\text{cm}^2$  to  $\text{m}^2$ ) passive light collection and illumination systems to be created. The thin optically transparent sheet is a monolithic (i.e. single material) micro-patterned polymer membrane constructed by bonding two or more functionalized thin layers with slightly different indices of refraction. Through careful selection of the transparent materials and appropriate design of the micro-optical elements, it is possible to control the direction of light rays entering, propagating through, and exiting the functionalized optical sheet. In general, the geometry and spatial distribution of micro-optical elements imprinted on the constituent layers of the sheet determines whether the light guide system acts as a large area concentrator, regional diffuser, or near ‘lossless’ light transmitter. Typical applications for large-area optical sheets include flexible illuminators and light-harvesting systems for wearable technology, creative indoor lighting, non-planar solar energy collectors, customized signature lighting, and enhanced safety illumination for motorized vehicles.

Most existing large-area optical light guide systems are mechanically rigid flat solar energy concentrators [1, 2] and backlight illumination panels for electronic displays [3–9]. These light collectors and illuminators are constructed from optically transparent thermoplastics (e.g. acrylic) or glass and fabricated using very expensive manufacturing methods (e.g. photolithography) that ensure precision light guidance through the microstructures for optimal performance and maximum efficiency. The exposed surface of the flat light collectors, or light harvesters, is typically patterned with an array of microlenses that focus incident light rays onto micro-prisms imprinted on the opposing surface [1, 2, 10–12]. The micro-prism elements then reflect the light rays back into the transmission by total internal reflection (TIR). The light rays propagate through the lower ‘core’ to the concentrator edge where it exits or strikes a photovoltaic (PV) cell [1, 8]. Similarly, rigid illumination panels act as light diffusers by utilizing various patterns of reflecting

\*Corresponding authors: George K. Knopf, The University of Western Ontario, London, ON, Canada, e-mail: gkknopf@uwo.ca. <http://orcid.org/0000-0002-8696-9247>; and Evgueni Bordatchev, National Research Council of Canada, London, ON, Canada, e-mail: Evgueni.Bordatchev@nrc-cnrc.gc.ca

Chloë Nicholson-Smith: The University of Western Ontario, London, ON, Canada. <http://orcid.org/0000-0002-9682-9889>

micro-elements [3, 13–15] to produce either uniform or signature lighting [3].

The same underlying design principles and techniques used to create rigid light collectors and illumination panels can be modified for developing flexible polymer optical sheets like those illustrated in Figure 1. Yeon et al. [15] extended these basic principles to develop a flexible light diffuser that had been patterned with inverse cone features. The diffusing micro-elements would disrupt or frustrate the path of the propagating light rays such that they would exit the core and emanate at the desired location from the diffuser surface. However, the complexity of the optical design problem is increased because the non-rigid light guide thickness and embedded micro-elements (e.g. micro-lens, prisms, pyramids, and wedges) can bend, stretch, and even fracture under extreme mechanical stress. In other words, small changes or distortions may significantly reduce the performance efficiency of the elastomeric light guide system.

To illustrate this concept of flexible optical sheets for a broad group of applications, the impact of key design parameters on the controlled guidance of light through a two-layer polydimethylsiloxane (PDMS) concentrator-transmitter-diffuser optical sheet is investigated using Zemax OpticStudio (Zemax LLC, Kirkland, WA, USA) ray tracing simulation and analysis software [16]. The proposed multi-functional PDMS optical sheet [17, 18] is fabricated from optically transparent PDMS and manufactured using soft-lithography techniques based on replica molding [19, 20]. Moldable PDMS has high optical transmittance properties (>95%) over the visible and near-infrared regions of the spectrum, and the index of refraction of the individual layers can be controlled by either modifying either the ratio of base-to-curing agent

[21, 22], adjusting the curing temperature, applying deep ultra-violet irradiation, or adding high refractive index nanoparticles such as titanium dioxide [23, 24]. The viscoelastic properties of the thermosetting PDMS also make it a suitable material for accurately producing the inverse pattern of the micro-elements imprinted on the casting mold [21, 25]. In this manner, the individual layers can be molded separately and then bonded together using oxygen plasma or corona discharge bonding. The fabrication of flexible optical sheets is a separate area of research and beyond the scope of this paper [21, 22, 25].

The design of the multifunctional concentrator-transmitter-diffuser optical sheet is summarized in Section 2. The performance measures for the light guide system include concentrator-transmitter efficiency ( $\eta_{c,t}$ ), combined concentrator-transmitter-diffuser efficiency ( $\eta_{c,t,d}$ ), and the percent uniformity of diffuser illumination ( $U_d$ ). These measures are, however, dependent upon a number of factors including optical sheet curvature ( $\kappa$ ) and the relative orientation of incident light source. As the curvature and characteristics of the incident light source can vary significantly between different applications, implementations for similar applications, or over time for the same arrangement, it is necessary to place constraints on the analysis and simulations. In this regard, the parametric analysis initially considers a flat ( $\kappa = 0$ ) PDMS optical sheet exposed to a collimated light source. Section 3 examines the key design parameters such as refractive indices for the two constituent layers, sheet thickness, active surface area, and geometric parameters for the various optical elements (lenses, coupling pyramids, reflecting prisms). The performance of the flat optical sheet under different parametric conditions is summarized in Section 4. The impact of sheet curvature ( $\kappa > 0$ ) on both system efficiency and

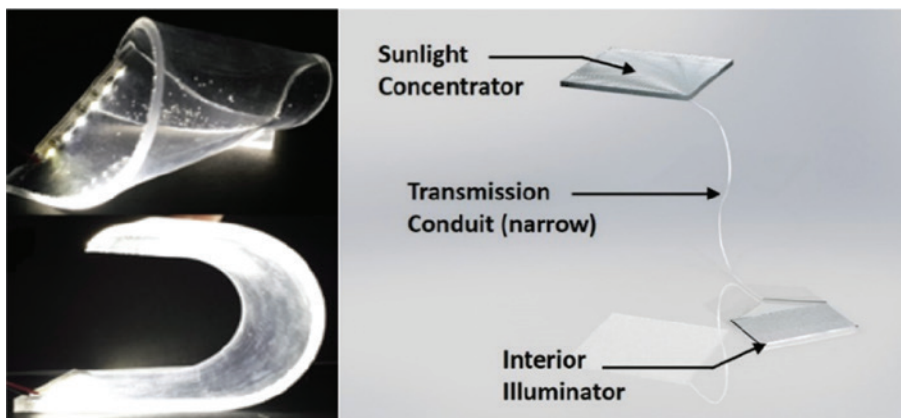


**Figure 1:** Large-area elastomeric optical sheets for reconfigurable illumination (left) and passive indoor lighting where a concentrator-transmitter-diffuser structure captures sunlight and transmits it to an interior room (right).

illumination uniformity is then briefly discussed. Finally, the concluding remarks and discussion on future work are presented in Section 5.

## 2 Multifunctional optical sheet

As the geometry and spatial distribution of micro-optical elements are application dependent, it is not possible to consider all cases. Rather, the goal is to closely examine the impact of the design parameters on the light guidance behavior through a combined concentrator-transmitter-diffuser PDMS optical sheet (Figure 2) using ray tracing software. The central region of the multifunctional optical sheet acts as a concentrator, or light collector, and is constructed from two superimposed PDMS layers with slightly different indices of refraction and layer thicknesses. The top layer is patterned with micro-lenses that focus the incident light rays onto the micro-pyramid

features imprinted on the bottom surface of the second layer (Figure 3). The micro-pyramids act as couplers, which reflect the rays and direct them to the edge of the concentrator region. The difference in index of refraction between the first ( $n_1$ ) and second layer ( $n_2$ ) ensures that the light rays striking the pyramid propagate laterally toward the concentrator edges by total internal reflection (TIR). The material properties of PDMS are assumed to be homogeneous with no optical absorption or volume scattering for the analysis. The lateral propagation of the light rays toward the diffuser represents light guide transmission functionality. The boundary region around the concentrator region of the light guide acts as a light diffuser (i.e. illuminator). The bottom face of the PDMS layer for the diffusing region is patterned with triangular-wedge-shaped features that run the full width of the light guide. These optical wedges are angled such that when the propagating rays strike the micro-element surface, they are reflected at an angle that causes the rays to be refracted out of the illuminating region. The wedges run along the

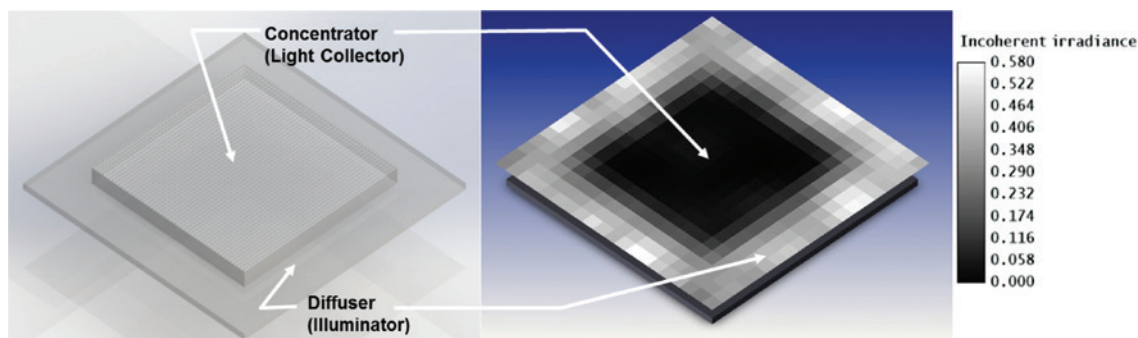


**Figure 2:** Simple multifunctional optical sheet with a combined concentrator (center), transmitter (beneath), and diffuser (border) regions. Note that the thickness of the layers comprising the optical sheet has been exaggerated for display purposes.

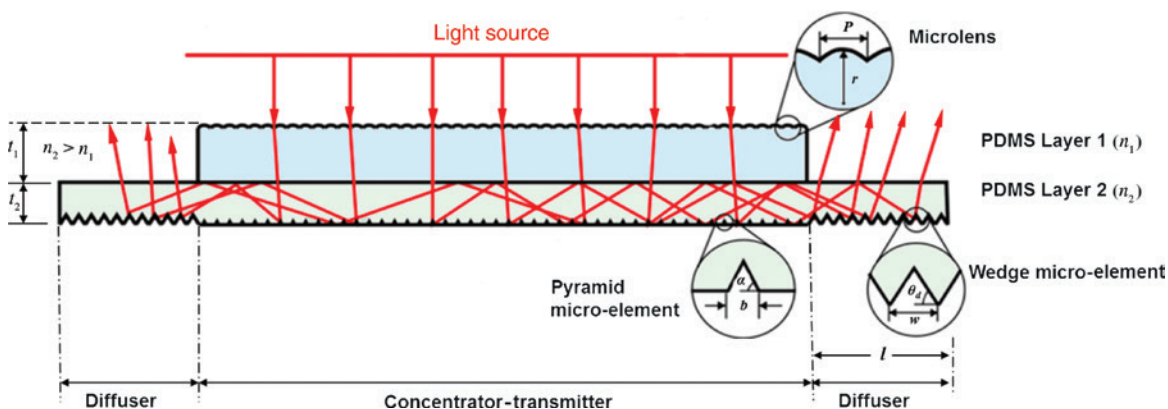


**Figure 3:** Cross-sectional view of a two-layer PDMS concentrator-transmitter-diffuser optical sheet. The incident light is focused onto the coupling pyramids by the micro-lens array and directed to the illuminating region where the light is diffused out of the device by wedge micro-elements.

length of the optical sheet and join at  $45^\circ$  with the wedges originating from the orthogonal directions. Note that in a realistic scenario, the light rays entering the device would largely be non-direction, diffuse, and dependent upon the surface orientation of the optical sheet. As the optical sheet is a flexible membrane that can be positioned in any orientation with respect to the incident light rays, it is not feasible to undertake an optical design process that satisfies all possible conditions. It is, therefore, sufficient to initially consider a single case such as a collimated light source positioned directly above the optical sheet. Note that the actual efficiencies and performance characteristics of a fabricated flexible optical sheet will always be less than the ‘ideal’.

The role of the concentrator-transmitter region of the multifunctional optical sheet (Figure 3) is to collect the incident light and focus it on the tip of the coupling pyramids where it is propagated outward toward the diffuser section. The effectiveness and efficiency of the concentrator [26] depends on the geometry and position of the micro-lenses in Layer 1 and the light-coupling pyramid structures embedded in Layer 2 (Figure 4). The sheet thickness ( $t_1 + t_2$ ), concentrator surface area (SA), and concentration ratio [11] must also be considered when designing the light concentrator. The concentration ratio of the light guide is given by the concentrator surface area, where the light enters (input), divided by the sum of the area of the concentrator faces, where the light exits (output).

The diffuser region at the border of the concentrator incorporates a series of reflective wedge features, which re-direct the light rays out of the optical sheet. The angles at which the propagating rays strike the sloped face of the micro-wedge determine how the light refracts out of the

sheet. The micro-wedge shape, as shown in Figure 3, is governed by angle  $\theta_d$  that is small enough for the transmitted light ray to be reflected, but large enough, such that the same ray can exit upon reflection [27]. From a functionality perspective, both the efficiency and the uniformity of illumination become important design considerations. The attributes of the diffuser region are affected by the shape, size, and spatial distribution of the wedge elements.

The performance of the optical sheet in terms of efficiency in collecting light rays, transmitting the rays to the edges or diffusing the captured rays is also dependent upon the optical sheet curvature ( $\kappa$ ) and the relative orientation of incident light source with respect to the sheet surface. It is necessary to place constraints on the analysis and simulations because the curvature and characteristics of the incident light source can vary significantly between different applications, implementations for similar applications, or over time for the same arrangement. In this regard, the parametric study initially considers a flat ( $\kappa = 0$ ) PDMS optical sheet exposed to a collimated light source. Once designed, the concentrator-transmitter-diffuser is analyzed in terms of changes in sheet curvature ( $\kappa > 0$ ). When the optical sheet is bent to a particular radius of curvature, the constituent microstructures are deformed and re-oriented with respect to the light source. These dimensional changes may introduce high optical losses due to frustrated TIR and, therefore, a significant drop in efficiency. To investigate the changes in efficiency, the optical sheet is assumed to bend in only one direction, and the sheet curvature ( $\kappa$ ) is defined as the reciprocal of the bending radius  $R$ , and given as

$$\kappa = 1/R \quad (1)$$

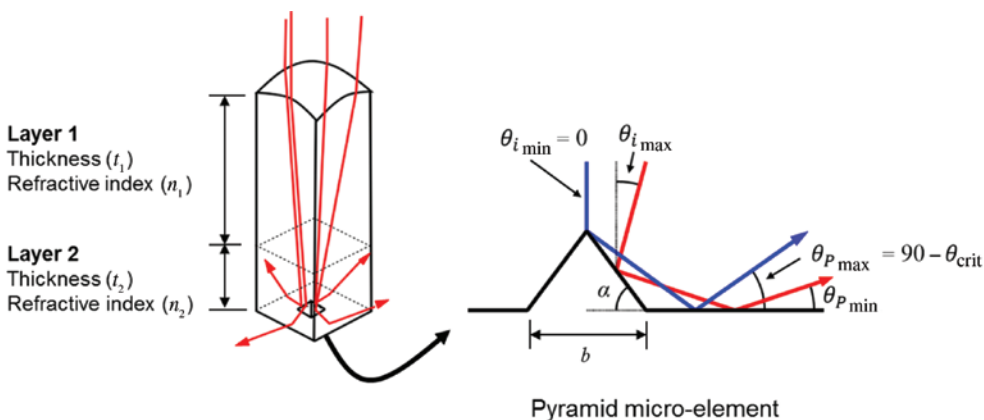


**Figure 4:** The primary function of the concentrator-transmitter region of the optical sheet where micro-lens array focus the incident light rays onto the coupling pyramids, which reflect the rays at an angle such that they are confined to Layer 2 for lateral transmission.

Note that multi-directional bending (i.e. twisting) is possible with the flexible optical sheet, but the losses will significantly increase.

### 3 Design parameters for an elastomeric optical sheet

The optical sheet design must ensure that the concentrator, transmitter, and diffuser regions function in unison, and therefore, the parameters must be determined simultaneously to achieve the desired light guidance properties. In this regard, the desired focal length ( $f$ ) of the concentrator micro-lenses will determine the maximum thickness ( $t_{\max} = t_1 + t_2$ ), of the two bonded PDMS layers. In addition, the thickness of the bottom light transmission layer ( $t_2$ ) must be selected to enable efficient re-direction of light rays to the concentrator edges and then onto the diffusion region for illumination. Furthermore, the refractive indices for the two constituent PDMS layers must be selected to ensure TIR.

To reduce the number of variables and unknowns when designing an optical sheet, it is necessary to impose constraints such as the refractive indices ( $n_1$ ) and ( $n_2$ ) for the two constituent PDMS layers, maximum sheet thickness ( $t_{\max}$ ), active area of the concentrator region ( $SA$ ), and minimum concentration factor ( $CF$ ) [17]. Once these parameters have been defined, the thicknesses of the individual layers can then be estimated as

$$t_2 = \sqrt{SA / CF} \quad (2a)$$

$$t_1 = t_{\max} - t_2 \quad (2b)$$

The physical constraints ( $n_1, n_2, t_{\max}, SA, CF$ ) imposed on the concentrator region of the optical sheet are then used to determine the key design parameters for the micro-elements in the concentrator, transmitter, and diffuser regions of the light guide system. Critical design parameters for the concentrator are the radius ( $r$ ) and pitch ( $P$ ) of the micro-lenses and the angle of incline ( $\alpha$ ) and base width ( $b$ ) of the coupling pyramids. The coupling pyramid parameters  $\alpha$  and  $b$  also determines the lateral transmission behavior of the light collector. The key design parameters for the diffuser region are the face angle ( $\theta_d$ ), diffuser length ( $l$ ), and width ( $w$ ) of the micro-wedge elements. The following section describes the key parameters for designing the micro-elements in the concentrator-transmitter ( $r, P, t_1, \alpha, b, t_2$ ) and the diffuser ( $\theta_d, l, w$ ) regions based on geometric optics. With some design

discretion, these parameters are scalable in terms of the layer thicknesses and active surface areas.

#### 3.1 Concentrator-transmitter design

The key design parameters for the micro-lens are the lens radius ( $r$ ) and pitch ( $P$ ). The pitch is the lens spacing, and the lenses can be arranged in either a rectangular (equally spaced) or hexagonal grid pattern. The focal length ( $f$ ) of each lens is determined by the maximum thickness of the optical sheet (i.e.  $f = t_{\max}$ ). Based on the classic lens maker's equation [28], the radius ( $r$ ) of the individual micro-lens in the array can be estimated as

$$r = t_{\max} (n_1 - 1) / n_1 \quad (3)$$

This estimation is possible because the difference between  $n_1$  and  $n_2$  is typically  $\Delta n \leq 0.15$ .

For the pyramid optical elements shown in Figure 4, the maximum allowable angle of propagation ( $\theta_{p_{\max}}$ ) for the impinging light rays is limited by the critical angle between the constituent layers as dictated by their refractive indices and can be given by

$$\theta_{p_{\max}} = 90 - \sin^{-1}(n_1 / n_2) \quad (4)$$

Although this equation accurately defines the maximum angle of propagation for total internal reflection in the light guide, it is based on assumptions not universally true for flexible optical sheets because any variation in the angle of the rays or optical sheet curvature will result in significant losses. For example, if an optical sheet with some surface curvature is required (i.e.  $\kappa > 0$ ), then, the angle of propagation ( $\theta_p$ ) should be significantly lower than the maximum allowable value ( $\theta_{p_{\max}}$ ). Unfortunately, reducing  $\theta_p$  may result in a significantly longer overall diffuser length.

The pitch ( $P$ ) of the micro-lenses dictates the angle of incidence ( $\theta_i$ ) where a small  $P$  results in a low  $\theta_i$  and, consequently, a higher density of coupling pyramids in the bottom layer. From a design perspective, the selection of minimum angle of incidence ( $\theta_{i_{\min}}$ ) and maximum angle of incidence ( $\theta_{i_{\max}}$ ) are application dependent. If the elastomeric optical sheet exhibits curvature, then, it will be necessary to increase the density of coupling pyramids and design for a small  $\theta_i$ . For most applications, the angle of incidence will range from  $0^\circ < \theta_i < 5^\circ$ .

Based on the ray path and the desired angle of propagation, the maximum allowable angle ( $\alpha_{\max}$ ) of the coupling pyramid is calculated as [17]

$$\alpha_{\max} = 0.5(\theta_{p_{\max}} + 90) \quad (5)$$

Based on the selected  $\theta_{i_{\max}}$  and the critical angle between the lower layer of the light guide and the surrounding medium, the minimum angle ( $\alpha_{\min}$ ) is determined as

$$\alpha_{\min} = \sin^{-1}(n_1/n_2) + \theta_{i_{\max}} \quad (6)$$

where  $n_0$  is the index of refraction of the surrounding medium (air), and  $n_2$  is the index of refraction of the PDMS Layer 2. In terms of design, the base angle ( $\alpha$ ) for the coupling pyramids must be  $\alpha_{\min} \leq \alpha \leq \alpha_{\max}$ . For an optical sheet with a surface curvature,  $\alpha \rightarrow \alpha_{\min}$ , whereas for a flat sheet,  $\alpha \approx (\alpha_{\min} + \alpha_{\max})/2$  is often used.

As the pitch of the concentrating micro-elements is based on the maximum angle of incidence of the rays on the coupling pyramids and the lens' radius ( $r$ ), the pitch ( $P$ ) can be calculated iteratively according to [17]

$$\theta_{i_{\max}} = \sin^{-1} \left( \frac{n_1}{n_2} \sin \left( \tan^{-1} \left( \frac{P/2}{\sqrt{r^2 - (P/2)^2}} \right) \right) - \sin^{-1} \left( \frac{1}{n_1} \sin \left( \tan^{-1} \left( \frac{P/2}{\sqrt{r^2 - (P/2)^2}} \right) \right) \right) \right) \quad (7)$$

The shape of the coupling micro-pyramids is dependent on the functionality of the concentrator, and the pyramid size must be minimized to reduce decoupling losses. Ideally, the rays would focus at a single point; however, due to the use of layers with different refractive indices and spheric lenses, which result in some focal shift, the focal width depends on the feature geometry. Although the focal width will dictate the minimum feature size for the coupling prisms, the relationship between feature size and wavelength must also be considered. For this light guide system, it was determined that the minimum feature dimension should not be less than 10 times the wavelength of visible light or approximately 0.01 mm.

Another important consideration is the relationship between their size and pitch. The efficiency of the concentrator is highly dependent on the proportion of its surface area occupied by coupling features, as this corresponds with the likelihood of a ray decoupling. In order to maintain a sufficiently high concentrator efficiency, the coupling feature base width  $b$  should not exceed 1/10 of the pitch or  $b_{\max} = 0.1 \times P$ . Note that no matter how precisely the coupling pyramid is designed, the selected fabrication methods will likely introduce geometric errors such as rounded apex and edges or fillets instead of sharp

transitions. These geometric errors can significantly alter the paths of the light rays.

### 3.2 Diffuser design

The diffuser incorporates a series of wedge elements, which reflect light off the angled surface causing the rays to refract out of the optical sheet. The efficiency and uniformity of illumination are affected by the shape, size, and spatial distribution of the wedges. The wedge face must be tilted at an angle small enough that the incident light is reflected off the features, but large enough that the ray is diffused out of the illuminating surface. The diffuser wedge angle can be calculated based on the geometry of the pyramid element in the concentrator because these structures dictate the propagation angle of rays in both the concentrator and diffuser. Based on wedge element geometry (Figure 5), the minimum and maximum propagation angles ( $\theta_{p_{\min}}, \theta_{p_{\max}}$ ) are

$$\theta_{p_{\min}} = 2\alpha - 90 - \theta_{i_{\max}} \quad (8)$$

$$\theta_{p_{\max}} = 2\alpha - 90 \quad (9)$$

where  $\alpha$  is the base angle for the coupling pyramids, and  $\theta_{i_{\max}}$  is the maximum angle of incidence of the concentrated rays on the coupling pyramids [Eq. (7)].

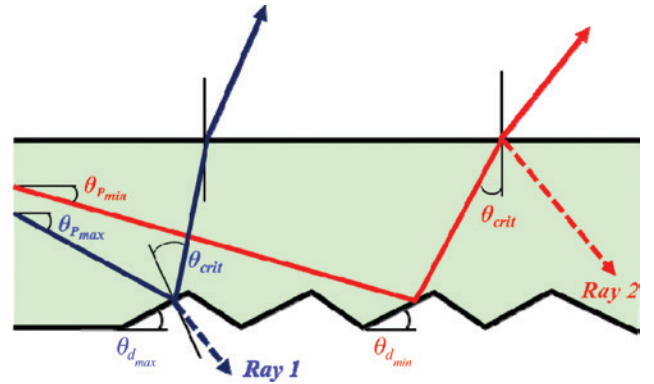


**Figure 5:** Ray diagram, which illustrates the minimum and maximum angles of propagation required to ensure the rays are properly diffused out the face of the illuminating region. If a light ray propagates at an angle greater than  $\theta_{p_{\max}}$ , or the diffuser angle exceeds  $\theta_{d_{\max}}$ , the ray (i.e. Ray 1) will refract out the bottom face. In contrast, if a light ray propagates at an angle less than  $\theta_{p_{\min}}$ , or the diffuser angle exceeds  $\theta_{d_{\min}}$ , the ray (i.e. Ray 2) will not be diffused. Note that the illustration does not take into account transmission losses that occur at the interface between two media with different refractive indices (i.e. Fresnel reflection).

Subsequently, the minimum and maximum diffuser angles can be calculated from the corresponding angles of propagation and the refractive index of the diffuser material ( $n_2$ ) and can be determined as

$$\theta_{d_{\min}} = 0.5 \left( 90 - \sin^{-1} \left( \frac{1}{n_2} \right) - \theta_{p_{\min}} \right) \quad (10)$$

$$\theta_{d_{\max}} = 90 - \sin^{-1} \left( \frac{1}{n_2} \right) - \theta_{p_{\max}} \quad (11)$$

A larger angle will ensure that rays are diffused closer to the normal of the illuminating face. However, an angle closer to the mid-range will improve efficiency by diffusing rays, which propagate at angles slightly higher or lower than the predicted values. For a non-planar optical sheet, a mid-range value is ideal as it will help ensure reflection off the wedge features and refraction out the illuminating face for variations in curvature. In this regard, an upper mid-range diffuser wedge angle of  $\theta_d = 30^\circ$  is typically used.

The minimum diffuser length ( $l_{\min}$ ) is calculated based on the shortest distance required for all rays to strike a diffusing wedge element only once. The minimum length is dependent on the wedge angle  $\theta_d$ , and the thickness of the diffuser layer,  $t_2$ , where

$$l_{\min} = 2 \left( \frac{t_2}{\tan \theta_{p_{\min}}} \right) \quad (12)$$

Finally, the diffuser wedge size,  $w$ , must be determined. The size of the wedge element is application dependent where a large  $w$  is more appropriate for a flexible optical sheet than a rigid light guide. For more uniform illumination on a flat diffuser, it was observed that the wedge height should be 1/10 of the layer thickness ( $t_2$ ). Therefore, the wedge width for the angle  $\theta_d$  can be calculated as

$$w = \frac{t_2}{(5 \times \tan \theta_d)} \quad (13)$$

## 4 Performance of the PDMS optical sheet

The Zemax OpticStudio ray tracing software is used to initially evaluate the performance of a flat ( $\kappa=0$ ) concentrator-transmitter-diffuser optical sheet. The impact of sheet curvature ( $\kappa > 0$ ) on both optical sheet efficiency

and illumination uniformity is then considered. For this study, the concentrator-transmitter diffuser optical sheet was modeled as a square light collector surrounded by an illuminating border region as shown in Figure 2. The geometric design of the physical three-dimensional optical sheet was created on SolidWorks and then imported as a STEP file into a ray-tracing software. The diffuser wedges were designed to exhibit maximum illumination in the middle of the boundary region with no significant light emission at the corners. An external rectangular light source was selected for simulations because it allowed the analyst to define the position, orientation, and wavelength of the incident illumination. Finally, a set of detectors was defined to quantify the optical sheet's output and evaluate its performance. It is necessary to note, however, that this analysis does not consider volume scattering and material absorption as these effects can be significant in real materials and large panels.

The pre-defined constraints on the molded PDMS sheet were  $n_0=1.0$ ,  $n_1=1.4$ ,  $n_2=1.55$ ,  $t_{\max}=2$  mm,  $SA=50\,000$  mm<sup>2</sup>, and  $CF=500\times$ . Based on the desired  $t_{\max}$  of the optical sheet, the individual layer thickness was determined [Eq. (2)] to be  $t_1=0.382$  mm and  $t_2=1.6$  mm. From the above equations, the design parameters associated with the micro-lens and coupling pyramids were calculated to be  $r=0.57$  mm,  $P=0.371$  mm,  $\alpha=52.5^\circ$ , and  $b=0.01$  mm. Similarly, the parameters associated with the diffuser wedges were determined to be  $\theta_d=30^\circ$ ,  $l=4.7$  mm, and  $w=0.144$  mm. Details on the calculations can be found in Appendix A.

To estimate the efficiency of the light guide system, the power from the light source was set to 1 W, and the total power detected in the concentrating edges and diffusing region were then measured. The efficiency of the concentrator-transmitter ( $\eta_{c-t}$ ) is defined by the ratio of light exiting the edges of the light-collecting region ( $I_{c-t}$ ) and total light entering the active concentrator surface ( $I_s$ ),

$$\eta_{c-t} = \frac{I_{c-t}}{I_s} \times 100. \quad (14)$$

Similarly, the efficiency of the combined concentrator-transmitter-diffuser ( $\eta_{c-t-d}$ ) is the ratio of the light detected at all illuminated diffuser surfaces ( $I_d$ ) and total light entering the concentrator surface ( $I_s$ ),

$$\eta_{c-t-d} = \frac{I_d}{I_s} \times 100. \quad (15)$$

For the simulations, the Zemax photo-detectors were placed above the diffuser region to measure the light exiting the face into air.

Another important measure of performance is the uniformity of illumination produced by the diffuser region. The total power across the diffuser region as measured by the Zemax detectors was divided by the total area of the diffuser, to estimate the average irradiance of the light guide in  $W/cm^2$ . The peak irradiance is identified from the detector data, and the average irradiance was divided by the peak irradiance to estimate the percent uniformity for the illumination from the diffuser using

$$U_d = \frac{I_{d_{avg}}}{I_{d_{peak}}} \times 100, \quad (16)$$

where  $U_d$  is the percentage of uniformity over the diffuser region,  $I_{d_{avg}}$  is the average diffuser irradiance, and  $I_{d_{peak}}$  is the peak diffuser irradiance.

Based on these performance measures, a parametric analysis of the various micro-elements in the concentrator and diffuser is now conducted in order to identify the design parameters that provide greatest efficiency and uniformity. The parametric investigation consists of a repeated analysis of the same optical sheet, varying only one parameter at a time, in order to identify the impact this parameter has on sheet performance.

## 4.1 Concentrator-transmitter parameters

### 4.1.1 Indices of refraction ( $n_1, n_2$ ) and surface area (SA)

The impact of various refractive index ratios ( $n_2/n_1$ ) on the concentrator-transmitter efficiency ( $\eta_{ct}$ ) was first examined (Figure 6) in an effort to better define the role of selecting the elastomer material (i.e. PDMS) for the constituent layers. For this analysis, the material, sheet thickness, and micro-geometric elements of the light-collector

region were fixed at the values provided above. The simulations showed a significant drop in concentrator-transmitter efficiency for smaller refractive index ratios and a relatively high efficiency ( $\eta_{ct} \approx 97\%$ ) when  $n_2/n_1 > 1.07$ . This implies that only a small difference in index of refraction between Layer 1 and Layer 2 is required for TIR. This is an important observation because the index of refraction of PDMS can be changed within this range by adjusting the ratio of the base to the curing agent (i.e. a simple fabrication parameter). However, if the ratio of refractive indices for the application must be  $< 1.07$ , then, it will be necessary to modify the geometric parameters for the various optical elements in the concentrator-transmitter. It is also important to interpret the values in the context of an ideal concentrator-transmitter because the efficiency will drop due to the Fresnel reflection at the interface between two media with different refractive indices, and real optical materials have non-ideal transmission properties because of material absorption and volume scattering.

Another user defined constraint is the size of the active surface area (SA) for the concentrator region. As the optical sheet under investigation is assumed to be a square, the impact of the concentrator width ( $\sqrt{SA}$ ) on overall concentrator-transmitter efficiency ( $\eta_{ct}$ ) is now considered. The area of the concentrator (SA) was varied from 225  $mm^2$  to 250 000  $mm^2$ , and the corresponding computed efficiencies are shown in Figure 7. The results also show an approximately linear relationship, with a slope of  $-0.0394\%/mm$ , between concentrator width and light collector efficiency. The negative slope implies that the larger the optical sheet, the less efficient it becomes in collecting and transmitting light to the diffusion areas. For example, a 500  $mm \times 500$   $mm$  concentrator will exhibit an efficiency of only 80%. Because of the interactions with a larger number of coupling pyramids, the collected light rays from a larger concentrator-transmitter surface area will have longer transmission paths to the diffuser region

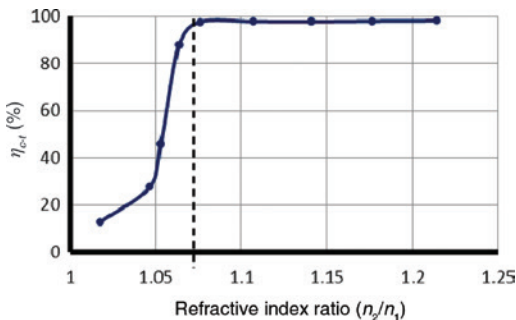


**Figure 6:** Impact of refractive index ratio ( $n_2/n_1$ ) on concentrator-transmitter efficiency ( $\eta_{ct}$ ). Note that these results were obtained under ideal conditions.

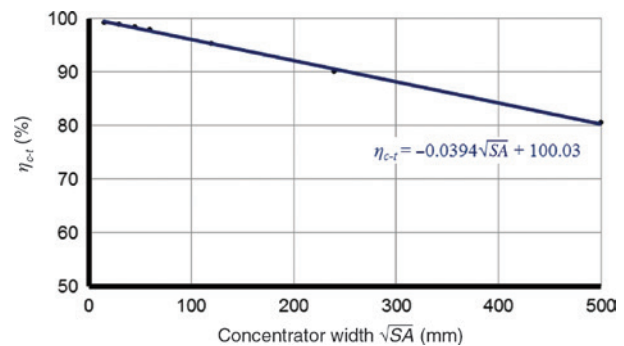


**Figure 7:** Impact of concentrator width ( $\sqrt{SA}$ ) on concentrator-transmitter efficiency ( $\eta_{ct}$ ).

and, thereby, a greater opportunity to prematurely escape the light guide system.

#### 4.1.2 Micro-lens pitch ( $P$ ) and radius ( $r$ )

The ideal pitch ( $P$ ) for the micro-lens array is based on the desired angle of incidence ( $\theta_i$ ) of the rays on the coupling pyramids. The ‘best’ angle based on preliminary analysis was  $5^\circ$ , but there is a broader range of acceptable angles that could have been selected. The micro-lens in the concentrator of the optical sheet is, therefore, modeled for values  $0.010 \leq P \leq 0.808$  mm, corresponding to  $0^\circ \leq \theta_i \leq 7^\circ$ . The relationship between the lens pitch and concentrator efficiency is examined in order to understand the impact of these variations (Figure 8). The highest efficiency was exhibited for  $P = 0.371$  mm. This is the pitch for where the coupling pyramids were optimized for desired conditions, and all collected rays could successfully be coupled into the lower layer of the optical sheet. For  $0.15 < P < 0.371$  mm, the efficiencies were relatively high ( $>90\%$ ) because the coupling pyramids are still able to reflect all incident rays by TIR. However, when the pitch becomes excessively small (i.e.  $P \ll 0.15$  mm), the increased density of elements causes a rapid drop in efficiency. Note that when  $P > 0.4$  mm the collector efficiency will also drop rapidly.

It is also important to consider the impact of small variations in the micro-lens radii ( $r$ ) on the concentrator-transmitter efficiency (Figure 8). The radius is selected to ensure that the light rays strike the pyramid elements that are located a distance  $t_{\max}$  (i.e. focal length) from the top surface of the optical sheet. Consequently, any variations to the radius or sheet thickness due to optical sheet stretching will result in a measurable change to the focal length ( $f$ ) and a significant drop in  $\eta_{ct}$  because the collected rays will fail to strike the pyramid features at the desired location and angle. Furthermore, the changes in  $r$  and  $t_{\max}$  increase the spot size of the concentrated light causing some rays to strike adjacent pyramids or prematurely exiting the concentrator-transmitter light guide structure. Based on the analysis, an ideal  $r = 0.57$  mm. Note that any design changes to the lens radius must be made in conjunction with either a change in layer thickness ( $t_{\max}$ ) or an increase in the size of the coupling pyramids.

#### 4.1.3 Coupling pyramid parameters ( $\alpha$ , $b$ )

The geometry of the coupling pyramids is also investigated in relation to  $\eta_{ct}$  (Figure 9, left). For the simulation study, the base angles of the pyramidal elements were varied between  $35^\circ \leq \alpha \leq 65^\circ$ . For the given design parameters,

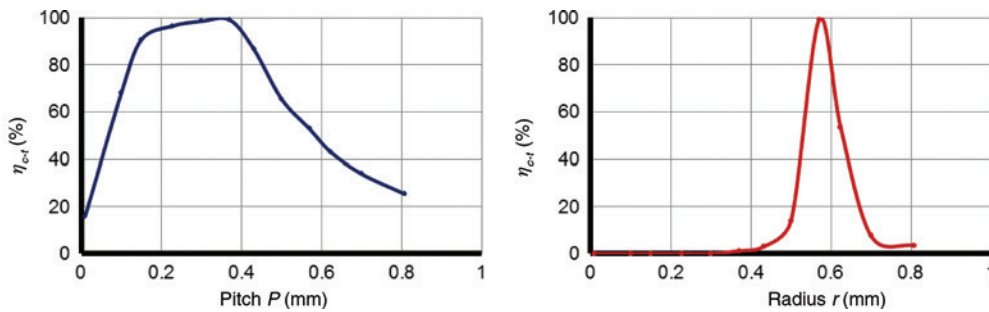


Figure 8: Impact of micro-lens parameters ( $P$ ,  $r$ ) on concentrator-transmitter region’s efficiency ( $\eta_{ct}$ ).

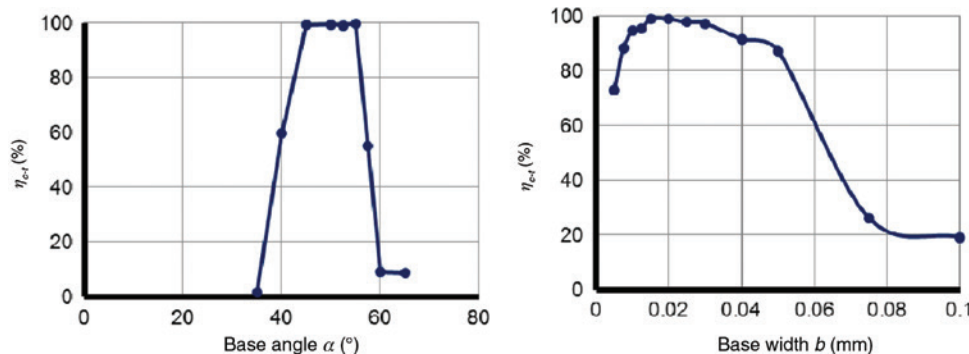


Figure 9: Impact of the coupling pyramid base angle ( $\alpha$ ) and width ( $b$ ) on concentrator-transmitter efficiency ( $\eta_{ct}$ ).

it was determined that an acceptable range of base angle for the pyramid elements are  $\alpha_{\min} = 45.2^\circ$  and  $\alpha_{\max} = 57.7^\circ$ . There is a near-linear decrease in efficiency for angles outside the range (both above and below). The reason that  $\eta_{ct} \neq 0$  for  $\alpha > 60^\circ$  is that some light rays are able to reflect off the lens in Layer 1 and propagate laterally through the light guide. Although any angle in the acceptable range could be selected, it is often beneficial to select  $\alpha$  at mid-range to ensure that the concentrator-transmitter accepts the wide possible variations in incident ray angles.

Similarly, the variations in pyramid base width from  $0.005 \leq b \leq 0.1$  mm were simulated (Figure 9, right). The results indicate that  $\eta_{ct} > 90\%$  can be achieved if the pyramid base width is in the range  $0.01 < b < 0.04$  mm. For coupling pyramids smaller than  $\sim 0.01$  mm, the physical optical element will be smaller than the area of the projected resulting in some rays refracting out the transmitter bottom. In contrast, if the pyramids become too large, then, they will interfere with laterally propagating rays and fail to reach the edges of the concentrator-transmitter region.

## 4.2 Diffuser parameters

Variations to the diffuser refractive index ( $n_2$ ) and diffuser micro-element geometry ( $\theta_d, l, w$ ) are also considered. The evaluation of performance will be based on the concentrator-transmitter-diffuser efficiency ( $\eta_{ct-d}$ ) and diffuser illumination uniformity ( $U_d$ ). It is necessary to look at the efficiency from the diffused illumination from the light that was originally collected by the concentrator region because an optical sheet is an integrated three-dimensional light guide system.

### 4.2.1 Refractive index ( $n_2$ ) of light diffuser

The impact of the variations in refractive index ( $n_2$ ) of the elastomeric layer on the diffuser performance is now considered. The refractive index was varied from  $1.42 \leq n_2 \leq 1.7$  as shown in Figure 10. The simulation results show a threshold of  $n_2 \sim 1.55$  for maximum efficiency ( $\eta_{ct-d}$ ). A larger refractive index will also provide the required optical element reflection and necessary diffusion for illumination. The uniformity of illumination exiting the diffuser ( $U_d$ ) is also impacted by the layer's refractive index. Although the uniformity appears to be optimized for a low refractive index, with a relatively steep drop-off preceding the optimized refractive index, the actual variation between the minimum and maximum uniformity is only

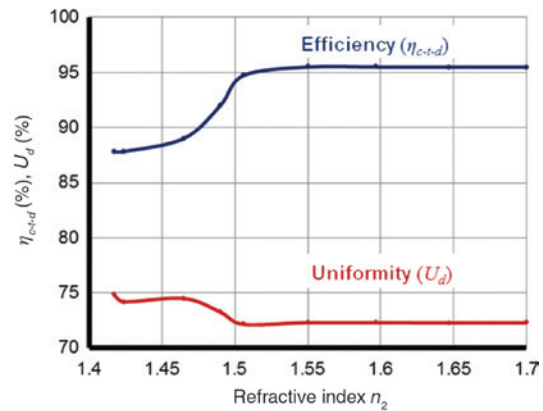


**Figure 10:** Impact of refractive index  $n_2$  on the concentrator-transmitter-diffuser efficiency ( $\eta_{ct-d}$ ) and diffuser illumination uniformity ( $U_d$ ).

2%, while the range in efficiency is 10%, so in most cases, it would be preferable to sacrifice some uniformity to achieve a significantly higher efficiency. The best performing diffuser allows rays to exit the layer at an angle approaching the normal to the active surface; however, by increasing the refractive index, the diffusion angle will decrease, presumably decreasing its uniformity as well (Figure 10).

### 4.2.2 Diffuser wedge angle ( $\theta_d$ )

Both the efficiency ( $\eta_{ct-d}$ ) and uniformity ( $U_d$ ) are also dependent on the angle ( $\theta_d$ ) wedge element in the diffuser region (Figure 11). Efficiency and uniformity values are relatively high for  $20^\circ \leq \theta_d \leq 35^\circ$ . While the results were predictable, there were some anomalies in the data relating to the diffuser angles greater than the recommended

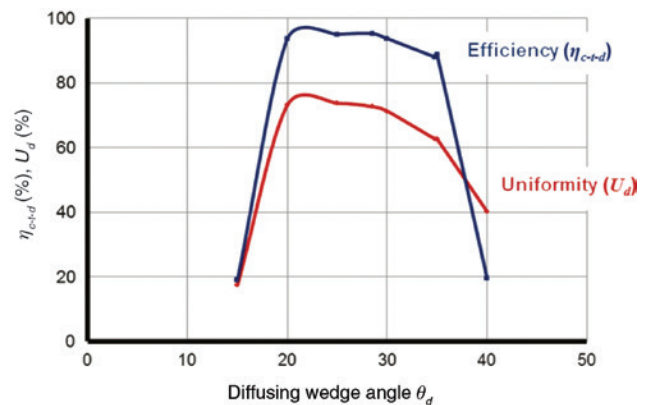


**Figure 11:** Impact of diffusing wedge angle  $\theta_d$  on the concentrator-transmitter-diffuser efficiency ( $\eta_{ct-d}$ ) and diffuser illumination uniformity ( $U_d$ ).

maximum  $\theta_{d_{\max}}$ . An anomaly was observed for  $\theta_d \approx 45^\circ$  (not shown), where efficiency actually increased and then dropped again with a slight increase in the wedge angle. The anomaly may be the result of the light rays, which are refracted out of the diffusing features, striking the opposite side of the wedge features and being refracted back into the light guide.

#### 4.2.3 Diffuser wedge width ( $w$ ) and length ( $l$ )

The dimensional width ( $w$ ) and length ( $l$ ) of the wedge features also played a role in the efficiency and illumination uniformity. The impact of the optical wedge widths in the range of  $0.025 \leq w \leq 1.5$  mm was simulated in the Zemax OpticStudio software and displayed in Figure 12. The simulations show a strong negative correlation between the wedge element size and the concentrator-transmitter diffuser efficiency ( $\eta_{c-t-d}$ ), exhibiting a near-linear relationship with a slope  $\approx -13\%/mm$ . This effect appears to be the result of light rays reflecting off the bottom face of the concentrating region and striking the first diffuser element at  $\theta_p > \theta_{p_{\max}}$ . The amount of illumination affected by this phenomenon appears to be directly proportional to the size of the first wedge element in the diffuser region. The simulations also show a negative relationship (slope  $\approx -39\%/mm$ ) between the illumination uniformity and the width of the wedge element. However, smaller wedge sizes exhibited a higher degree of uniformity because these elements were able to distribute the light more evenly across the illuminating face.

Furthermore, the length of the diffusing region must also be considered when designing a hybrid optical sheet that functions as a light collector, transmitter, and illuminator. Figure 13 shows the impact of the length parameter

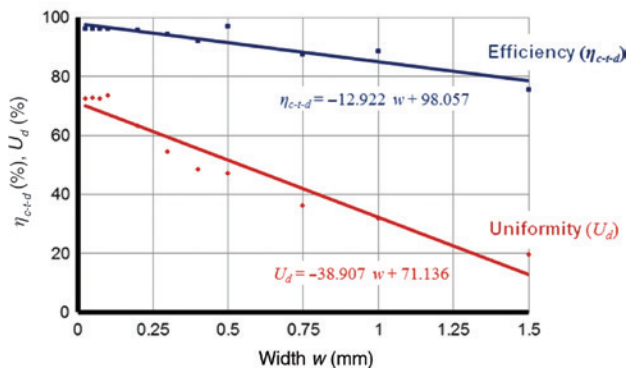


**Figure 12:** Impact of micro-wedge width ( $w$ ) on the concentrator-transmitter-diffuser efficiency ( $\eta_{c-t-d}$ ) and diffuser illumination uniformity ( $U_d$ ).

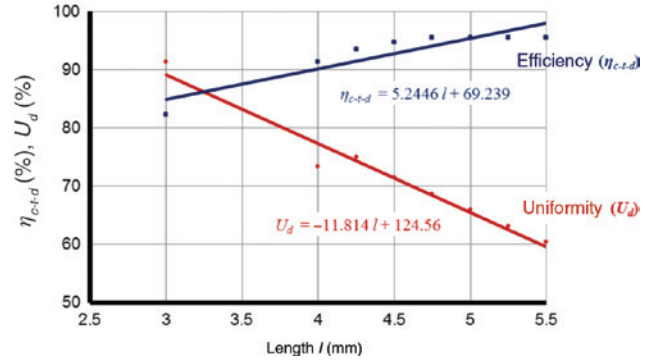


**Figure 13:** Impact of micro-wedge length ( $l$ ) on the concentrator-transmitter-diffuser efficiency ( $\eta_{c-t-d}$ ) and diffuser illumination uniformity ( $U_d$ ).

( $l$ ) on the concentrator-transmitter-diffuser efficiency and the illumination uniformity of the diffuser region. For this study, the range of length values was  $3 \leq l \leq 5.5$  mm. The variations in length affected the diffuser performance according to the predictions; however, some notable trends emerged. The increase in efficiency is approximately linear (slope  $\approx 5.2\%/mm$ ) with respect to diffuser length as is the decrease in illumination uniformity (slope  $\approx -12\%/mm$ ). The increase in efficiency arises, in part, because a longer diffuser will increase the likelihood of a light ray striking a diffusing wedge and refracting out the illuminating face. However, this same process will cause a corresponding decrease in uniformity because the number of rays remaining in the light guide will decrease with distance from the concentrator-transmitter edge reducing the uniformity of light emission. The ideal length of the wedge element is a balance between efficiency and desired uniformity. However, if a higher degree of either uniformity or efficiency is desirable, then the length may need to be adjusted accordingly.

### 4.3 Impact of curvature on optical sheet performance

The concentrator-transmitter-illuminator optical sheet is now analyzed in terms of changes in sheet curvature ( $0 < \kappa < 1$ ). The parameters of the micro-elements in the concentrator-transmitter ( $r, P, t_1, \alpha, b, t_2$ ) and the diffuser ( $\theta_d, l, w$ ) regions are based on the discussion above. The pre-defined constraints on the soft molded PDMS sheet are  $n_0 = 1.0, n_1 = 1.4, n_2 = 1.55, t_{\max} = 2$  mm,  $SA = 50\,000$  mm<sup>2</sup>, and  $CF = 500\times$ . Based on the desired  $t_{\max}$  of the optical sheet, the individual layer thicknesses are  $t_1 = 0.382$  mm and  $t_2 = 1.6$  mm. From micro-element geometry and ray optics,

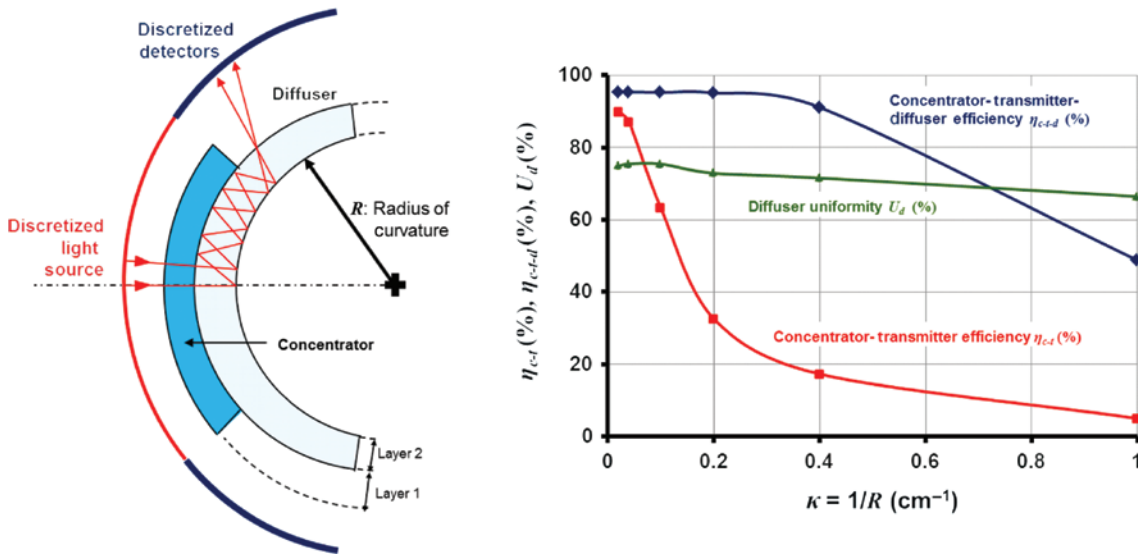


**Figure 14:** Cross-section of curved multifunctional optical sheet (left) and the impact of curvature ( $\kappa$ ) on observed efficiencies and diffuser uniformity (right).

the design parameters associated with the micro lens and coupling pyramids are calculated to be  $r=0.57$  mm,  $P=0.371$  mm,  $\alpha=52.5^\circ$ , and  $b=0.01$  mm. Similarly, the parameters associated with the diffuser wedges are determined to be  $\theta_d=30^\circ$ ,  $l=4.7$  mm, and  $w=0.144$  mm. A rectangular collimated light source (1 W) is selected for the simulations because it allows the analyst to define the position, orientation, and wavelength of the incident illumination. Finally, a set of simulated detectors is used to quantify the optical sheet’s output and evaluate its performance.

Figure 14 is a simplified drawing of the cross-section for the curved optical sheet (left) and the corresponding

efficiencies and uniformity responses for varying curvatures ( $\kappa$ ) (right). The results are for an incident light source that lies parallel to the curved surface geometry. Note that prior to bending,  $\kappa=0$ , the concentrator-transmitter and diffuser regions exhibit efficiencies ( $\eta_{ct}$ ,  $\eta_{ct-d}$ ) less than 100% because of the geometry and spatial distribution of the imprinted micro-features. Under these design conditions, the analysis shows that  $\eta_{ct}$  drops significantly for  $\kappa > 0.05$  cm<sup>-1</sup>, while  $\eta_{ct-d}$  exhibits a drop around  $\kappa > 0.2$  cm<sup>-1</sup>. It is also important to note that the uniformity of illumination exhibited by the diffuser bending ( $U_d \approx 70\%$ ) does not change significantly over bending because of the

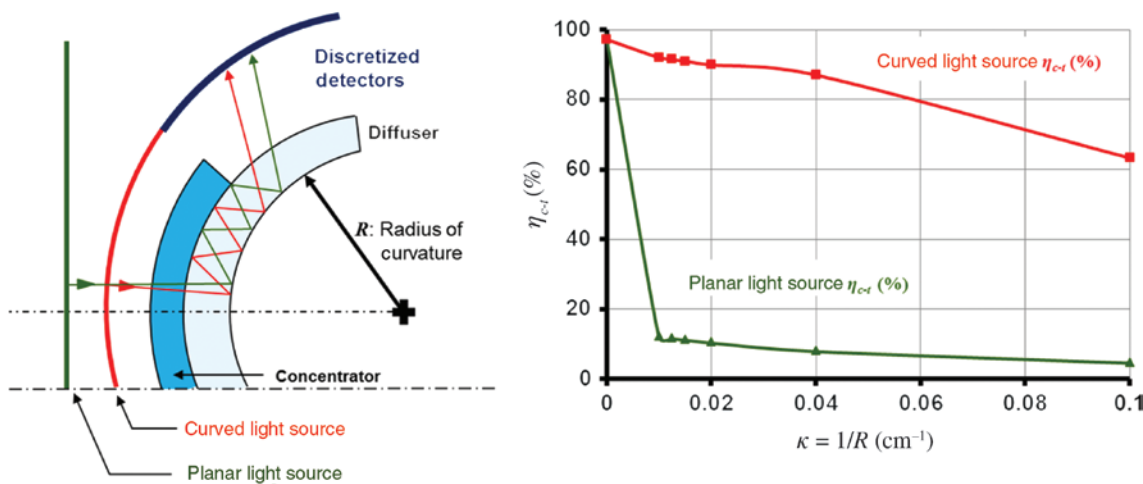


**Figure 15:** Cross-section of curved concentrator-transmitter region (left) and relationship between the concentrator-transmitter efficiency ( $\eta_{ct}$ ) and curvature ( $\kappa$ ) for planar and curved external lighting (right).

shape and spatial distribution of the micro-wedges. These observations imply that the most critical parameters for designing a bendable multifunctional optical sheet are associated with the microstructures in the concentrator-transmitter region ( $r, P, \alpha, b$ ). Any significant deformation or misalignment between the coupling micro-lens and micro-pyramids will alter the focal point ( $f$ ) and angle of incidence ( $\theta$ ) and, consequently, overall efficiency. Optimization is not always possible or feasible from either the design or fabrication perspective because of the requirement for a flexible large-area ( $\text{cm}^2$  to  $\text{m}^2$ ) elastomeric optical sheet.

The location and orientation of the external light source is also a critical factor when analyzing the performance of bendable optical sheets. For passive light-collecting and -harvesting systems, the light rays can strike the micro-lenses from any undetermined direction, and therefore, optimization for all scenarios is impossible. To investigate the impact of external lighting on concentrator-transmitter performance, two cases were considered: planar and curved light sources. The planar light source is reminiscent sunlight or overhead lighting, whereas the curved light source follows the shape of the optical sheet. Figure 15 shows the change in efficiency ( $\eta_{c,t}$ ) for both light sources. As the curvature increases, the efficiency of the optical sheet to the stationary planar light source drops rapidly to  $\eta_{c,t} < 10\%$ . The impact of curvature is significantly less if the light rays emanate from the curved light source. As the light source is often undefined, it is clear that the bendable optical sheet will always perform less than ideal no matter what microstructures or dimensional parameters are used.

## 5 Discussion

In this study, ray tracing software was used to simulate and examine the impact of key material and optical micro-element geometry on the efficiency of light guidance through a flat two-layer PDMS optical sheet that acts as a combined light collector, near-lossless transmitter and area illuminator. The optical engineer's design requirements for the light collector ( $n_1, n_2, t_{\max}, SA, CF$ ) are used to determine the key design parameters for the micro-elements in the concentrator-transmitter ( $r, P, t_1, \alpha, b, t_2$ ) and the diffuser ( $\theta_d, l, w$ ) regions of the multifunctional optical sheet. The light guidance behavior of the various optical sheet regions is evaluated in terms of concentrator-transmitter efficiency ( $\eta_{c,t}$ ), combined

concentrator-transmitter-diffuser efficiency ( $\eta_{c,t,d}$ ), and the percent uniformity of diffuser illumination ( $U_d$ ).

The ray tracing software can only assist the engineer in making an appropriate design decision. However, the large number of parameters for this design problem is interdependent such that a small change in one parameter will have a profound effect on multiple properties of the optical sheet. It is necessary, therefore, to impose design constraints, which reduce the number of unknowns or the acceptable range of the variables. In this regard, the underlying assumption was that the optical sheet was flat with an infinite radius of curvature ( $\kappa=0$ ). The design of the curved optical sheets is a separate topic and can be investigated by reviewing the work by Nicholson-Smith [17]. Furthermore, the designer must identify the physical constraints imposed by the selected materials and available fabrication processes. The choice of material for this research was optically transparent PDMS because the index of refraction can be controlled by adjusting the ratio of base-to-curing and the fabrication of each constituent layer could be achieved through soft molding [21]. The constraints imposed by the fabrication method can be highly restrictive, but necessary, if the multifunctional optical sheet is to be very large ( $\text{cm}^2$  to  $\text{m}^2$ ) and mechanically flexible (i.e. non-rigid).

The properties of the external light source also play a critical role in parameter selection and assessing optical sheet performance in terms of efficiency or desired output characteristics (e.g. uniform illumination at the desired region of the sheet). For a flat collector-transmitter-diffuser optical sheet ( $\kappa=0$ ) receiving light from a planar collimated source, the overall efficiency of the best performing design was over 90%. However, the same optical sheet when significantly bent ( $\kappa \gg 0$ ) produced an efficiency of  $\sim 5\%$ . The large number of variables also implies that there is no single optimal solution for designing a mechanically flexible optical sheet. Rather, the parametric design equations and simulation results must be viewed with caution. From the design perspective, it is better to look at ranges and relative relationships between the key parameters. It is also important to understand that the solution will always be less than optimal because of the number of interrelated parameters, dimensional scale, and uncontrolled light source.

## 6 Summary

Mechanically flexible elastomeric optical sheets are large-area light guide systems that provide engineers with new

opportunities to create innovative light collection and illumination systems for passive indoor lighting, non-rigid light-harvesting systems, customized signature lighting, and enhanced safety lighting. The optically transparent sheet is a monolithic polymer membrane that can be draped on flat or arbitrarily curved surfaces. The thin optically transparent sheet is a monolithic (i.e. single material) micro-patterned polymer membrane that can be draped over an arbitrarily shaped surface. The membrane is a light guidance system with an active surface area ranging from a few cm<sup>2</sup> to several m<sup>2</sup> constructed by bonding two or more functionalized thin layers with slightly different indices of refraction. By careful selection of the transparent materials and design of micro-optical features, it is possible to control the direction of light rays entering, propagating through, and exiting the functionalized optical sheet.

The ray tracing software was used to examine the impact of a key material and optical micro-element geometry on the efficiency of light guidance through these non-rigid systems, a soft molded two-layer PDMS optical sheet. The analysis initially involved a flat ( $\kappa=0$ ) PDMS optical sheet with specific regions for light collection (concentration), transmission, and illumination (diffusion). The light guidance behavior of the optical sheet, under different parameter conditions, was investigated in terms of concentrator-transmitter efficiency ( $\eta_{c,t}$ ), combined concentrator-transmitter-diffuser efficiency ( $\eta_{c-t-d}$ ), and the percent uniformity of diffuser illumination ( $U_d$ ). The simulation study showed that carefully selected parameters under ideal external lighting conditions could result in  $\eta_{c-t-d} \approx 90\%$  and  $U_d \approx 70\%$ . Clearly, these efficiencies and diffuser illumination characteristics can be significantly reduced under non-ideal conditions or using optical elements with geometric dimensions outside the recommended ranges. The impact of sheet curvature ( $\kappa > 0$ ) on both system efficiency and illumination uniformity was also examined. The study showed that the concentrator-transmitter efficiencies dropped significantly with a modest curvature ( $<10\%$ ), but the diffuser region remains  $>60\%$  efficient for a large curvature ( $\kappa \rightarrow 1$ ). Future work will focus on ‘optimizing’ the performance of the concentrator-transmitter-diffuser optical sheet and exploring the impact of dimensional scaling on the system performance.

**Acknowledgments:** This paper is the result of the collaboration between the University of Western Ontario (London, Ontario, Canada) and the National Research Council of Canada (London, Ontario, Canada). Partial financial support was also provided by the Natural Sciences and Engineering Research Council (NSERC) of Canada, Funder

Id: 10.13039/501100000038, Grant Number: RGPIN/05858-2014. The authors would also like to acknowledge the support of CMC Microsystems (Kingston, Ontario, Canada) in providing access to the Zemax OpticStudio software through their Designer subscription program.

## Appendix A

As discussed in Section 4, the pre-defined constraints on the two-layer PDMS optical sheet were  $n_0=1.0$ ,  $n_1=1.4$ ,  $n_2=1.55$ ,  $t_{\max}=2$  mm,  $SA=50\,000$  mm<sup>2</sup>, and  $CF=500\times$ . Based on the desired  $t_{\max}$  of the optical sheet, the remaining parameters for the Zemax OpticStudio simulation were determined from the equations in Section 3. A summary of the calculations is provided below.

$$t_2 = \frac{\sqrt{SA}}{CF} = \frac{\sqrt{50000}}{500} = 0.4 \text{ mm} \quad (\text{A1})$$

$$t_1 = t_{\max} - t_2 = 2.0 - 0.4 = 1.6 \text{ mm} \quad (\text{A2})$$

$$r = \frac{t_{\max}(n_1 - 1)}{n_1} = \frac{2(1.4 - 1)}{1.4} = 0.57 \text{ mm} \quad (\text{A3})$$

$$\theta_{p_{\max}} = 90 - \sin^{-1}\left(\frac{n_1}{n_2}\right) = 90 - \sin^{-1}\left(\frac{1.4}{1.55}\right) = 25^\circ \quad (\text{A4})$$

$$\alpha_{\max} = \frac{\theta_{p_{\max}} + 90}{2} = \frac{25 + 90}{2} = 57.2^\circ \quad (\text{A5})$$

$$\alpha_{\min} = \sin^{-1}\left(\frac{n_0}{n_2}\right) + \theta_{i_{\max}} = \sin^{-1}\left(\frac{1}{1.55}\right) + 5 = 45.2^\circ \quad (\text{A6})$$

where  $\theta_{i_{\max}}$  is assumed to be  $5^\circ$  and  $n_0=1$  (i.e. air). The selected base angle  $\alpha$  is mid-range or

$$\alpha = \frac{\alpha_{\max} + \alpha_{\min}}{2} = \frac{57.2^\circ + 45.2^\circ}{2} = 52.5^\circ \quad (\text{A7})$$

$$\theta_{i_{\max}} = \sin^{-1}\left(\frac{n_1}{n_2} \sin\left(\tan^{-1}\left(\frac{P/2}{\sqrt{r^2 - (P/2)^2}}\right)\right) - \sin^{-1}\left(\frac{1}{n_1} \sin\left(\tan^{-1}\left(\frac{P/2}{\sqrt{r^2 - (P/2)^2}}\right)\right)\right)\right) \quad (\text{A8})$$

Substitute known parameters into Eq. (A8) such that

$$5 = \sin^{-1} \left( \frac{1.4}{1.55} \sin \left( \tan^{-1} \left( \frac{0.5P}{\sqrt{(0.57)^2 - (0.5P)^2}} \right) \right) - \sin^{-1} \left( \frac{1}{1.4} \sin \left( \tan^{-1} \left( \frac{0.5P}{\sqrt{(0.57)^2 - (0.5P)^2}} \right) \right) \right) \right)$$

and solve for the single unknown pitch, where  $P = 0.371$  mm in this example.

$$b_{\max} = \frac{P}{10} = \frac{0.371}{10} = 0.0371 \text{ mm} \quad (\text{A9})$$

$$\theta_{p_{\min}} = 2\alpha - 90 - \theta_{i_{\max}} = 2(52.5^\circ) - 90^\circ - 5^\circ = 10^\circ \quad (\text{A10})$$

$$\theta_{p_{\max}} = 2\alpha - 90 = 2(52.5^\circ) - 90^\circ = 15^\circ \quad (\text{A11})$$

$$\begin{aligned} \theta_{d_{\min}} &= \frac{1}{2} \left( 90 - \sin^{-1} \left( \frac{1}{n_2} \right) - \theta_{p_{\min}} \right) \\ &= \frac{1}{2} \left( 90 - \sin^{-1} \left( \frac{1}{1.55} \right) - 10 \right) = 20 \end{aligned} \quad (\text{A12})$$

$$\theta_{d_{\max}} = 90 - \sin^{-1} \left( \frac{1}{n_2} \right) - \theta_{p_{\max}} = 90 - \sin^{-1} \left( \frac{1}{1.55} \right) - 15 = 35^\circ \quad (\text{A13})$$

For this illustrative example, the diffuser wedge angle was selected above the mid-range, or  $\theta_d = 30^\circ$ .

$$l_{\min} = 2 \left( \frac{t_2}{\tan(\theta_{p_{\min}})} \right) = 2 \left( \frac{4.15}{\tan(10^\circ)} \right) = 4.7 \text{ mm} \quad (\text{A14})$$

$$w = \frac{t_2}{5 \times \tan(\theta_d)} = \frac{0.415}{5 \times \tan(30^\circ)} = 0.144 \text{ mm} \quad (\text{A15})$$

## References

- [1] S. Bouchard and S. Thibault, *Appl. Opt.* 51, 6848 (2012).
- [2] J. H. Karp, E. J. Tremblay and J. E. Ford, *Opt. Express* 18, 1122 (2010).
- [3] R. A. Ronny, G. K. Knopf, E. Bordatchev and S. Nikumb, *J. Micro/Nanolithogr. MEMS MOEMS* 12, 23002 (2013).
- [4] S. H. Baik, S. K. Hwang, Y. G. Kim, G. Park, J. H. Kwon, et al., *J. Opt. Soc. Korea* 13, 478–483 (2009).
- [5] W. J. Cassarly, in ‘Optical Design and Testing III’, *Proc. SPIE* 6834, 683407 (2007).
- [6] S. I. Chang, J. B. Yoon, H. Kim, J. J. Kim, B. K. Lee, et al., *Opt. Lett.* 31, 3016–3018 (2006).
- [7] P. H. Huang, T. C. Huang, Y. T. Sun and S. Y. Yang, *Opt. Express* 16, 15033–15038 (2008).
- [8] F. Meinardi, A. Colombo, K. A. Velizhanin, R. Simonutti, M. Lorenzon, et al., *Nat. Photonics* 8, 392–399 (2014).

- [9] J. W. Pan and Y. W. Hu, *Opt. Lett.* 37, 3726–3728 (2012).
- [10] J. H. Karp, E. J. Tremblay and J. E. Ford, in ‘Proc. Photovoltaic Specialists Conference’, Honolulu, HI, 493 (2010).
- [11] J. H. Karp and J. E. Ford, in ‘High and Low Concentrator Systems for Solar Electric Applications IV’, *Proc. SPIE*, 7407, 74070D (2009).
- [12] J. H. Karp, E. J. Tremblay, J. M. Hallas and J. E. Ford, *Opt. Express* 19, A673 (2011).
- [13] A. Gombert, B. Bläsi, C. Bühler, P. Nitz, J. Mick, et al., *Opt. Eng.* 43, 2525 (2004).
- [14] Y. Okuda and I. Fujieda, in ‘Advances in Display Technologies II’, *Proc. SPIE*, 8280, 82800W (2012).
- [15] J. Yeon, J. Lee, H. Lee, H. Song, Y. Mun, et al., *J. Micromech. Microeng.* 22, 095006 (2012).
- [16] Zemax OpticStudio LLC. OpticStudio, [Online]. Available: <http://www.zemax.com/os/OpticStudio> (2016).
- [17] C. O. Nicholson-Smith, Controlled guidance of light in large area flexible optical waveguide sheets, MSc thesis, The University of Western Ontario (2016).
- [18] C. Nicholson-Smith, G. K. Knopf and E. Bordatchev, *Proc. SPIE* 9759, 97590C–97590C (2016).
- [19] Y. Xia and G. M. Whitesides, *Angew. Chem. Int. Ed.* 37, 550–575 (1998).
- [20] S. K. Tang and G. M. Whitesides, in ‘Optofluidics: Fundamentals, Devices, and Applications’, Eds. By Y. Fainman, L. Lee, D. Psaltis and C. Yang (McGraw-Hill, 2009), 0071601562.
- [21] R. S. Green, Fabrication of large mechanically flexible multi-layered PDMS optical devices, MSc thesis, The University of Western Ontario (2016).
- [22] R. Green, G. K. Knopf and E. V. Bordatchev, *Proc. SPIE* 10101, 101010Y-1 (2017).
- [23] S. Lee, H. Shin, S. Toon, D. K. Yi, J. Choi, et al., *J. Mater. Chem.* 18, 1751–1755 (2008).
- [24] J. R. L. Little, Tunable and high refractive index polydimethylsiloxane polymers for label-free optical sensing, Master’s thesis, Queen’s University (2013).
- [25] R. Green, G. K. Knopf and E. Bordatchev, in ‘Advanced Fabrication Technologies for Micro/Nano Optics and Photonics IX’, *Proc. SPIE* 97590, 97590U (2016).
- [26] P. Xie, H. Lin, Y. Liu and B. Li, *Opt. Express* 22, A1389–A1398 (2014).
- [27] ‘Optical design tools for backlight displays,’ *Optical Research Associates*, <https://optics.synopsys.com/lighttools/pdfs/ToolsforBacklights.pdf> (2010).
- [28] R. E. Cohen, D. R. Lide and G. L. Trigg, in ‘AIP Physics Desk Reference’, 3rd ed, Chapter 19, (Springer/AIP Press, Optics New York, 2003) pp. 568–596.



**Chloë Nicholson-Smith**

The University of Western Ontario  
London, ON, Canada.

<http://orcid.org/0000-0002-9682-9889>

Chloë Nicholson-Smith works as a Research Associate for Canadian Surgical Technologies and Advanced Robotics at the University of Western Ontario. She received her MSc in Mechanical and

Materials Engineering from the University of Western Ontario in 2016 and received her BESC in 2014. Her current research focuses on the use of computer-aided engineering in the design and evaluation of medical devices.



**George K. Knopf**  
The University of Western Ontario  
London, ON, Canada  
[gkknopf@uwo.ca](mailto:gkknopf@uwo.ca)  
<http://orcid.org/0000-0002-8696-9247>

George K. Knopf is a Professor in the Department of Mechanical and Materials Engineering at The University of Western Ontario, Canada. His research activities involve bioelectronics, biosensors, laser material processing, and micro-optical transducers. Past contributions have led to novel imaging systems, innovative fabrication processes, and advanced materials. Dr. Knopf's current work involves the development of conductive graphene-derivative inks and novel fabrication processes for printing bioelectronic circuitry on mechanically flexible substrates. He has co-edited two CRC Press volumes entitled *Smart Biosensor Technology* and *Optical Nano and Micro Actuator Technology*, and recently co-authored a SPIE E-Book on *Biofunctionalized Photoelectric Transducers*. Professor Knopf has acted as a technical reviewer for numerous academic journals, conferences, and granting agencies and has co-chaired several international conferences.



**Evgueni Bordatchev**  
National Research Council of Canada  
London, ON, Canada  
[Evgueni.Bordatchev@nrc-cnrc.gc.ca](mailto:Evgueni.Bordatchev@nrc-cnrc.gc.ca)

Evgueni Bordatchev is a Senior Research Officer and a Team Leader for the Specialty Coating Microfabrication group at the National Research Council of Canada, in London, Ontario. He received his Master, PhD, and Doctor of Technical Science degrees in electro-mechanical engineering from Don State Technical University, Rostov-on-Don, Russia, in 1982, 1989, and 1996, respectively. Since 1998, he is with the National Research Council demonstrating his national and international recognition as an expert in laser/cutting-based high-precision micromachining, surface functionalization and polishing, micro-optics, micro-opto-electro-mechanical systems/sensors, and micro-molds/dies. He has authored/co-authored over 224 publications and holds six patents. Dr. Bordatchev is an Adjunct Professor at The University of Western Ontario (London, Ontario, Canada) since the year 2000, and he is also a member of the Editorial Board for Springer's Journal, *Lasers in Manufacturing and Materials Processing*.